ORIGINAL RESEARCH
published: 02 August 2019
doi: 10.3389/fncom.2019.00046

# A Closed-Loop Toolchain for Neural Network Simulations of Learning Autonomous Agents

*Jakob Jordan*[1,2*†], *Philipp Weidel*[2,3,4†] *and Abigail Morrison*[2,5]

[1] *Department of Physiology, University of Bern, Bern, Switzerland,* [2] *Institute of Neuroscience and Medicine (INM-6) & Institute for Advanced Simulation (IAS-6) & JARA-Institute Brain Structure Function Relationship (JBI 1/INM-10), Research Centre Jülich, Jülich, Germany,* [3] *aiCTX, Zurich, Switzerland,* [4] *Department of Computer Science, RWTH Aachen University, Aachen, Germany,* [5] *Faculty of Psychology, Institute of Cognitive Neuroscience, Ruhr-University Bochum, Bochum, Germany*

Neural network simulation is an important tool for generating and evaluating hypotheses on the structure, dynamics, and function of neural circuits. For scientific questions addressing organisms operating autonomously in their environments, in particular where learning is involved, it is crucial to be able to operate such simulations in a closed-loop fashion. In such a set-up, the neural agent continuously receives sensory stimuli from the environment and provides motor signals that manipulate the environment or move the agent within it. So far, most studies requiring such functionality have been conducted with custom simulation scripts and manually implemented tasks. This makes it difficult for other researchers to reproduce and build upon previous work and nearly impossible to compare the performance of different learning architectures. In this work, we present a novel approach to solve this problem, connecting benchmark tools from the field of machine learning and state-of-the-art neural network simulators from computational neuroscience. The resulting toolchain enables researchers in both fields to make use of well-tested high-performance simulation software supporting biologically plausible neuron, synapse and network models and allows them to evaluate and compare their approach on the basis of standardized environments with various levels of complexity. We demonstrate the functionality of the toolchain by implementing a neuronal actor-critic architecture for reinforcement learning in the NEST simulator and successfully training it on two different environments from the OpenAI Gym. We compare its performance to a previously suggested neural network model of reinforcement learning in the basal ganglia and a generic Q-learning algorithm.

**Keywords: closed-loop simulation, reinforcement learning, spiking neuronal networks, virtual environments, computational neuroscience**

OPEN ACCESS

***Edited by:***
*Mario Senden,*
*Maastricht University, Netherlands*

***Reviewed by:***
*Laurent U. Perrinet,*
*UMR7289 Institut de Neurosciences de la Timone (INT), France*
*Daniel Saunders,*
*University of Massachusetts Amherst, United States*

****Correspondence:***
*Jakob Jordan*
*jordan@pyl.unibe.ch*

*†These authors have contributed equally to this work*

***Received:*** *31 May 2019*
***Accepted:*** *25 June 2019*
***Published:*** *02 August 2019*

***Citation:***
*Jordan J, Weidel P and Morrison A (2019) A Closed-Loop Toolchain for Neural Network Simulations of Learning Autonomous Agents. Front. Comput. Neurosci. 13:46. doi: 10.3389/fncom.2019.00046*

## 1. INTRODUCTION

Simulation is a key component of modern neuroscience, constituting a third methodological pillar along with experiment and theory. Its uses include, but are not limited to, validation of theory, generation of hypotheses, production of surrogate data for data analysis tools, and discovery of structural and dynamical constraints for functional models. Thanks to a variety of initiatives, researchers now have access to well maintained, high performance simulators for all scales of neural systems from molecular simulations (e.g., STEPS; Wils and De Schutter, 2009) over complex neuron (e.g., NEURON, Carnevale and Hines, 2006; GENESIS, Bower and Beeman, 2007) and network models (e.g., NEST, Gewaltig and Diesmann, 2007; BRIAN, Goodman and Brette, 2009; NENGO, Bekolay et al., 2013, SINABS, Sheik and Liu, 2019) to whole brain simulations using neural fields (e.g., TVB, Sanz Leon et al., 2013).

In the realm of spiking neural networks, development of simulators has been largely driven by two viewpoints: the physical, concerned with the dynamics of individual neurons and networks of neurons (e.g. relationship of correlation structure to connectivity, bifurcation landscapes), and the electrophysiological, concerned with the response of neurons and networks to stimuli (e.g. PSTHs, response variability). Thus, spiking neural network simulators provide good support for constructing structured networks of neurons with a variety of dynamics, applying arbitrarily complex stimuli and recording the evolution of dynamic variables for later analysis.

However, restricting our inquiries to the dynamical and transformational properties of neuronal networks neglects large classes of fundamental and exciting neuroscientific questions. In particular, investigations of embodied cognition, of organisms operating autonomously in an environment and learning how to optimize their behavior within it, require a different approach. Firstly, it is crucial to simulate agents that interact with their environments, thereby actively shaping their future sensations rather than merely passively consuming experimentally provided stimuli (see e.g., Wilson, 2002). This necessitates a *closed-loop* set-up, in which the neuronal network can be conceived of as an autonomous agent within an environment. The neuronal network receives sensory stimuli from the environment, which alter its network dynamics. The resulting activity of the network, or of specific subnetworks of it can be interpreted as motor commands which alter the agent's configuration with respect to its environment (e.g., rotation, lateral movement) or the configuration of the environment itself (e.g., operation of levers or buttons). The change in configuration brings about a change in the sensory stimuli, and thus the neuronal network interacts with the environment in a continuous cycle. Depending on the scientific question, the network activity can also drive plasticity processes in the network, causing alterations in its own configuration, and thus in its response to sensory stimuli. In this way, new behavior can be learned through interaction with the environment, rather than through extensive exposure to labeled training data.

Secondly, it is important to establish a set of standardized benchmarks which allow alternative models to be compared with each other and good models to be improved and extended. With regard to this latter point, a comparison of the progress of the fields of machine learning, and learning in neuronal networks, provides a useful illustration. The last decade has witnessed major progress in the field of machine learning, moving from small-scale toy problems to large-scale real-world applications including image (Krizhevsky et al., 2012) and speech recognition (Hinton G. et al., 2012), complex motor-control tasks (Mnih et al., 2016), and playing (video) games at super-human performance (Mnih et al., 2015; Silver et al., 2016). This progress has been driven mainly by an increase in computing power, especially by training deep networks on graphics processing units (Raina et al., 2009), and conceptual breakthroughs like layer-wise pretraining (Hinton and Salakhutdinov, 2006; Bengio et al., 2007) or dropout (Hinton G.E. et al., 2012). Even so, this rate of progress would not have been possible without the wide availability of high-performance ready-to-use tools, e.g., Torch (Collobert et al., 2002), Theano (James et al., 2010), Caffe (Jia et al., 2014), TensorFlow (Abadi et al., 2016), and standardized datasets and environments for benchmarking, such as the MNIST (LeCun et al., 1998), CIFAR (Krizhevsky and Hinton, 2009), and ImageNET (Deng et al., 2009) datasets, and the MuJoCo (Todorov et al., 2012), ALE (Bellemare et al., 2015), and OpenAI Gym (Brockman et al., 2016) toolkits. While ready-to-use tools allow researchers to focus on important aspects rather than basic implementation details, standardized benchmarks have guided the community as a whole toward promising approaches, as for example in the case of convolutional networks through the ImageNET competition (Russakovsky et al., 2015).

Similarly, researchers in the field of computational neuroscience have benefited from the increase of computational power and achieved many conceptual breakthroughs over the last decade, with a plethora of new neuron, synapse and network models being developed. As mentioned above, a variety of simulators are available to the computational neuroscientist, yet so far no generally accepted set of benchmarks exist (but see Gerstner and Naud, 2009).

One particular area in which the lack of standardized benchmarks is apparent is research into reinforcement learning (RL) in neurobiological substrates. Inspired by behavioral experiments, RL is concerned with the ability of organisms to learn from previous experiences to optimize their behavior in order to maximize reward and avoid punishment (see e.g., Sutton and Barto, 1998). RL has a long tradition in the field of machine learning which has led to several powerful algorithms, such as SARSA and Q-learning (Watkins, 1989). Similarly, a large variety of neurobiological models have been proposed in recent years (Izhikevich, 2007; Potjans et al., 2009, 2011; Urbanczik and Senn, 2009; Vasilaki et al., 2009; Frémaux et al., 2010; Frémaux et al., 2013; Jitsev et al., 2012; Friedrich et al., 2014; Rasmussen and Eliasmith, 2014; Aswolinskiy and Pipa, 2015; Baladron and Hamker, 2015; Rombouts et al., 2015; Friedrich and Lengyel, 2016; Rueckert et al., 2016). However, only a small proportion of these rely on publicly available simulators and all of them employ custom built environments. Even for fairly simple environments, this has led to a situation where different network models are difficult to compare and reproduce, thus creating a fragmentation of research efforts. Instead of building upon and extending existing models, researchers are forced to spend too much time on recreating basic functionality for custom implementations.

The need for closed-loop simulation has led to the Human Brain Project (2014) (HBP) dedicating significant resources of a subproject (Neurorobotics) to the development of the necessary infrastructure that allows users to conduct robotic experiments in virtual environments and connect these to their neural network implementations with a web interface (Falotico et al., 2017). This approach specifically addresses the need of researchers developing neuronal or neuro-inspired controllers for robotic applications. A more pared-down approach, suitable for researchers who are primarily concerned with understanding the neural circuits, rather than controlling sophisticated robotic actuators, is provided by Weidel et al. (2016). This approach allows any neuronal network simulator that implements the MUSIC (Djurfeldt et al., 2010) interface (including NEST and NEURON) to be coupled with any robotic simulator implementing the ROS (Quigley et al., 2009) interface [including Gazebo (Koenig and Howard, 2004), Morse (Echeverria et al., 2011), or Webots (Michel, 2004)].

However, neither approach directly addresses the issue of the lack of standardized benchmarks for neuronal agents operating autonomously and learning to optimize their behavior in an environment. Such benchmarks exist: the OpenAI Gym (Brockman et al., 2016) provides a rich and generic collection of standardized RL environments developed to support the machine learning community in evaluating and comparing algorithms. All environments are accessible via a simple, unified interface, that requires an agent to supply an action and returns an observation and reward for its current state. The toolkit includes a range of different environments with varying levels of complexity ranging from low-dimensional fully discrete (e.g., *FrozenLake*[1]) to high-dimensional fully continuous tasks (e.g., *Humanoid*[1]). The consistency of the OpenAI Gym environments across different releases supports researchers in reproducing and extending previous work and allows systematic benchmarking and comparison of learning algorithms and their implementations. The easy accessibility of different tasks fosters progress by allowing researchers to focus on learning algorithms instead of basic implementation details of particular environments, and prompts researchers to evaluate the performance of their algorithms on many different tasks.

One possibility to access this set of benchmarks is to implement spiking networks in tools that are natively compatible with the OpenAI Gym, such as Tensorflow (Abadi et al., 2016) or PyTorch (Paszke et al., 2017). However, as the components of spiking neural network models (e.g., neuron and plastic synapse models, stimulation, and recording devices) are typically not shipped with these tools, this once again places the burden of implementation on the user (but see Hazan et al., 2018 for a spiking-neural network orientated approach). In particular, since these tools focus on machine learning applications rather than exploring biological intelligence, several critical features for computational modeling of learning in biological neuronal networks, such as few-compartment neurons, conductance-based synaptic interactions or neuromodulated plasticity, lie outside the scope of these libraries. Therefore, to make a comprehensive resource of benchmarks available to the computational neuroscience community, we developed a toolchain to interface neural network simulators with the OpenAI Gym. Using this toolchain, researchers can rely on well-tested, high-performance simulation engines for spiking neural networks to power their models, and evaluate them against a curated set of standardized environments, allowing more time to focus on neurobiological questions, such as the configuration and plasticity of neural circuits underlying exploration of the environment and exploitation of prior experience.

In the next section we introduce additional pre-existing components on which our toolchain relies, and afterwards discuss how it links the different tools. We demonstrate its functionality by implementing a neural actor-critic in NEST and successfully training it on two different environments from the OpenAI Gym.

## 2. PRE-EXISTING COMPONENTS

All network simulations in this manuscript are carried out with NEST[2] (Gewaltig and Diesmann, 2007), a neural simulator designed for the efficient simulation of large-scale networks of simple spiking neuron models with biophysically realistic connectivity. The simulation kernel scales from small simulations on a laptop to super computers, with the largest simulation to date containing about $10^9$ neurons and $10^{13}$ synapses, corresponding to about 10% of the human cortex at the resolution of individual cells and connections (Kunkel et al., 2014; Jordan et al., 2018). NEST is actively developed and maintained by the NEST initiative[3] in collaboration with the community, is freely available under the GPLv2 and is supported by the HBP with the explicit aim of widespread long-term availability and maintainability. The simulation set-up, e.g., definition of neurons and connections, can conveniently be performed via an interpreted language (e.g., PyNEST; Eppler et al., 2009) while the propagation of network dynamics is implemented in C++. OpenMP is used for node-local parallelization while MPI provides inter-node communication. While using a compiled language for the compute-intensive part provides significant performance gains compared to an interpreted language, it makes it less straightforward to interface the simulator with other tools not specifically designed for this.

The OpenAI Gym (Brockman et al., 2016) is a toolkit for reinforcement learning research focused on ease of use for machine learning researchers. An explicit goal of the OpenAI Gym is to compare different RL algorithms with each other in a consistent fashion. It provides a unified Python interface to a rich collection of curated RL environments, e.g., Atari games[4] or continuous control tasks for robotic applications[5].

An environment in the OpenAI Gym is updated in steps. In each step, the agent receives an observation representing the state of the environment, e.g., the agent's location within it, or other configurational information. This is typically a vector of real values. In addition, it receives a real-valued reward for entering the current environmental state. Depending on the environmental set-up, the reward may be zero for the majority of state transitions, and only non-zero (positive for rewards or negative for punishments) when the agent achieves a well-defined

[1]https://gym.openai.com/envs

[2]http://nest-simulator.org/

[3]https://nest-initiative.org/

[4]https://gym.openai.com/envs/#atari

[5]https://gym.openai.com/envs/#mujoco

goal. On the basis of the current state and its internal policy, the agent provides an action to the environment to trigger the next state transition. The reward can be used as information to adjust the agent's policy, such that its behavior in the environment evolves, typically such that it receives more reward in future trials in the same environment.

While the network implementation that we present in the results section relies on the NEST simulator, the toolchain can also be used with other simulators that support the MUSIC library, for example NEURON (Carnevale and Hines, 2006). The MUlti-SImulation Coordinator is a multi-purpose middleware for neural network simulators built on top of MPI (Message Passing Interface) that enables online interaction of different simulation engines (Djurfeldt et al., 2010). MUSIC takes care of starting all MUSIC-controlled executables (e.g., adapters and simulators) defined in a configuration file provided by the user in separate processes. During execution it makes sure that all processes evolve synchronously with a predefined real-time factor independent of the computational load of the individual processes (Moren et al., 2015). MUSIC provides named MPI channels, referred to as MUSIC ports, which allow the user to set up communication streams between several processes. While originally intented to distribute a single neural network model across different simulators, the MUSIC library can also be used to connect neural simulators to other applications.

For example, to connect neural simulators to robotic simulators, we recently developed the ROS-MUSIC Toolchain (RMT; Weidel et al., 2016) which provides an interface from MUSIC to the Robotic Operating System (ROS; Quigley et al., 2009). ROS is the most popular middleware in the robotic community and is able to interact with many robotic simulators and hardware platforms. The RMT allows exchange of well-defined messages between ROS and MUSIC via stand-alone executables, so called adapters, that were designed with a focus on modularity. The toolchain contains several different adapters each performing a rather simple operation on streams of inputs (e.g., filtering). By concatenating several adapters, the overall transformation of the original data can become more complex, for example converting high-dimensional continuous data (e.g., sensory data) to low-dimensional discrete data (e.g., action potentials) or vice-versa. More information and introductory examples can be found on GitHub[6].

## 3. RESULTS

To enable the online interaction of neural network simulators and the OpenAI Gym, we rely on two different libraries: MUSIC, to interface with the neural simulator, and ZeroMQ (Hintjens, 2013) to exchange messages with the environment simulated in the OpenAI Gym. In the following, we describe these two parts of the toolchain and demonstrate their functionality by interfacing a neural network simulation in NEST with two different environments.

### 3.1. Extending the ROS—MUSIC Toolchain

We extended the RMT by adding adapters that support communication via ZeroMQ following a publish-subscribe pattern. ZeroMQ is a messaging library that allows applications to exchange messages at runtime via sockets. Continuously developed by a large community, it offers bindings for a variety of languages including C++ and Python, and supports most operating systems. A single communication adapter of the RMT sends (receives) data via a ZeroMQ socket and receives (sends) data via a MUSIC port. While the adapters can handle arbitrary data, we defined a set of specialized messages in JSON format (see **Supplementary Material**) specifically designed to communicate observations, rewards, and actions as discrete or continuous real-valued variables of arbitrary dimensions, as used in the OpenAI Gym. We chose the JSON format due to its simplicity, easy serialization and broad platform support.

In addition to the ZeroMQ adapters dedicated for communication with MUSIC, we developed several further adapters that can perform specific transformations of the data. OpenAI Gym places few restrictions on the nature of the environment: it can be continuous or discrete with arbitrary dimensionality. Thus, in order to generate the required closed-loop functionality, the observations provided by the environment must be consistently transformed to a format that can be fed into neural network simulations. Conversely, the activity of the neural network must be interpreted and transformed into valid actions which can be executed in the environment.

A standard way to address the first issue with some degree of biological plausibility is to introduce a layer of *place cells* (Moser et al., 2008). Each of these cells is tuned to a preferred (multidimensional) observation, i.e., is highly active for a specific input and less active for other inputs (see e.g., Frémaux et al., 2013). The dependence of the activity of a single place cell on observations is described by its tuning curve, often chosen as a multidimensional Gaussian. To perform the transformation of observations to activity of place cells, we implemented a *discretize adapter* that allows users to specify the position and width of the tuning curves of an arbitrary number of place cells. One disadvantage of this approach is that the number of place cells required to cover the whole observation space evenly scales exponentially in the number of dimensions of the observation. For observations with a small number of dimensions, however, this approach is very suitable.

To perform action selection, we added several adapters that can, respectively, select the most active neuron (*argmax adapter*), threshold the activity across neurons to create a binary vector (*threshold adapter*), or linearly combine the activity of neurons across many input channels (*linear decoder*). Depending on the type of action required by the environment (discrete/continuous), the user can select a single one or a combination of these. Specifications of the adapters can be found in the documentation of the RMT[7].

In general, we followed the design principle behind the RMT and developed modular adapters. This makes each individual

[6]https://github.com/incf-music/ros-music-adapters

[7]https://github.com/incf-music/music-adapters

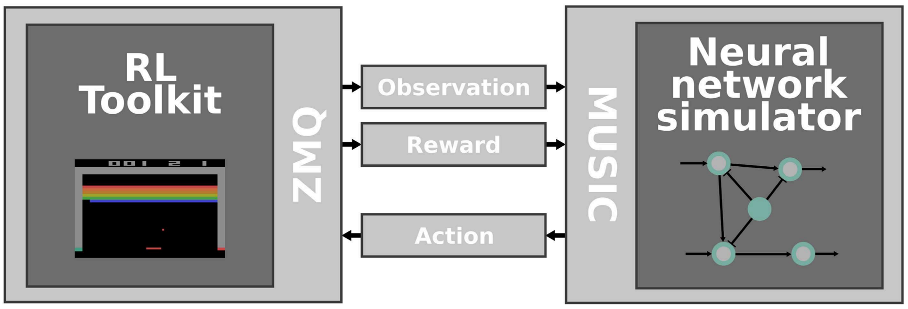

**FIGURE 1 |** Interfacing RL toolkits with neural network simulators. The RL toolkit **(left)** is responsible for emulating an environment that provides observations and rewards which are communicated via ZeroMQ sockets and MUSIC adapters **(middle)** to a neural network simulator **(right)**. Concurrently, the activity of the simulated neural network is transformed to an action and fed back to the RL toolkit.

adapter easy to understand and enables users to quickly extend the toolchain with their own adapters. By combining several adapters, the RMT allows arbitrarily complex transformations of the data and can hence be applied to many use-cases.

## 3.2. ZeroMQ Wrapper for the OpenAI Gym

The second part of the toolchain is a Python wrapper around the OpenAI Gym that exposes ZeroMQ sockets (Hintjens, 2013) for communicating actions, observations and rewards (see section 2 and **Figure 1**). The wrapper consists of four different threads that coordinate: (i) performing steps in an environment, (ii) receiving actions via a ZeroMQ SUB socket, (iii) publishing observations via a ZeroMQ PUB socket, and (iv) publishing rewards via a ZeroMQ PUB socket.

Before spawning the threads, the wrapper starts a user-specified environment and creates the necessary communication buffers. The thread coordinating the environment reads actions from the corresponding buffer, performs single steps in the environment and updates the observation and reward buffers based on the return values of the environment. Upon detecting that a single episode has ended, e.g., by an agent reaching a certain goal position, it resets the environment and allows a break of user-specified duration before starting the next episode.

The communication threads continuously send (receive) messages via ZeroMQ and read from/write to the corresponding buffers. All threads can be run with different update intervals, for example, to slow down movement of the agent by performing steps on a coarse time grid whilst continuously receiving action choices from the neural network simulation running on a fine time grid. The user can specify a variety of parameters via a configuration file in JSON format (see **Supplementary Material**). Detailed specifications of the wrapper can be found in the documentation.

In contrast to MUSIC-controlled executables, the ZeroQM wrapper is not started by the MUSIC library. As a result, the environment and the simulation evolve simultaneously but asynchronously. The simulator hence continuously receives input from the environment and vice versa. Due to the possibility of choosing a real-time factor for MUSIC-controlled processes, the user can easily achieve reliable interaction between the environments and the network simulation. The loosely coupled, asynchronous nature of the toolchain has the benefit that one could, for example, train the same network on a wide variety of different environments without stopping the simulation, in order to investigate transfer learning in spiking neural networks.

## 3.3. Applications

To demonstrate the functionality of the toolchain, we implemented a neural network in NEST and trained it on two different environments simulated in the OpenAI Gym. In the first task the agent needs to learn to perform a sequence of actions in order to reach the top of a hill in a continuous environment. The second task is a classical grid-world in which an agent needs to learn to navigate to a goal position in a two-dimensional discrete environment with obstacles. We first describe the neural network architecture and learning rule and afterwards discuss the network's performance on the two tasks.

### 3.3.1. Neural Network Implementation

We consider a temporal-difference learning algorithm (Sutton and Barto, 1998) implemented as an actor-critic architecture based on the spiking neuronal network proposed by Frémaux et al. (2013). For the purpose of demonstrating the toolchain, we simplified the model by replacing the spiking neuron models with rate neurons, thereby avoiding issues arising from noise introduced by spiking neuron models (Potjans et al., 2011; Frémaux et al., 2013). Note, however, that the toolchain is not restricted to rate-based models; any neuron model available in the neural simulators with MUSIC interfaces can be used.

The neuron dynamics we considered here are given by the following stochastic differential equation:

$$\tau \frac{dz_i(t)}{dt} = -z_i(t) + \mu_i + f\left(h_i(t) - \theta_i\right) + \xi_i(t), \qquad (1)$$

where $\tau$ is some positive time constant, $\mu_i$ a baseline activity level, $f(\cdot)$ some (arbitrary) activation function, $h_i(t)$ a time dependent input field, $\theta_i$ an input threshold and $\xi_i(t)$ Gaussian white noise with a certain standard deviation $\sigma_\xi$. The input field $h_i(t)$ is determined by the activity of other neurons according to $h_i(t) :=$

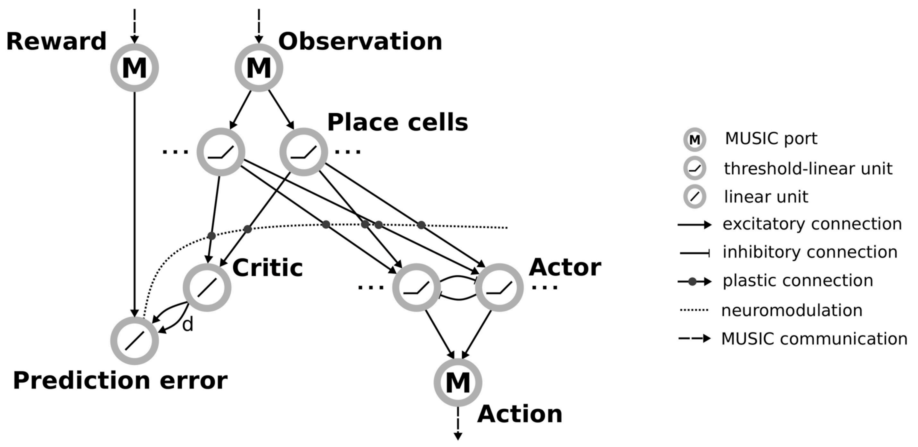

**FIGURE 2 |** Actor-critic architecture for reinforcement learning with rate neurons. Observations are communicated via a MUSIC input port to a population of place cells. These project both to a critic unit and to actor units arranged in a winner-take-all circuit. The critic and an additional MUSIC input port project to a unit representing the reward prediction error that modulates the plasticity between the place cells and their downstream targets, the critic and actors. The actor units project to a MUSIC output port encoding the selected action.

$\sum_j w_{ij} z_j(t)$, with $w_{ij}$ denoting the strength of the connection (weight) from neuron $j$ to neuron $i$. Here we will exclusively consider activation functions of the form $f(x) := x$ (linear case), and $f(x) := \Theta(x)x$ (threshold-linear case, "relu"). Here $\Theta(\cdot)$ denotes the Heaviside function, defined as

$$\Theta(x) := \begin{cases} 1 & x > 0 \\ 0 & \text{else} \end{cases} \tag{2}$$

Neuron dynamics are integrated in NEST on a fixed time-grid by a stochastic-exponential-Euler method with a step size determined by the resolution of the simulation. For more details on the neuron model implementation (see Hahne et al., 2017).

The input layer is a population of threshold-linear rate neurons which receive inputs through MUSIC and encode observations from the environment (see **Figure 2**). These place cells project via plastic connections to a single neuron representing the value that the network assigns to the current state (the *critic*). An additional neuron calculates the reward-prediction error by combining the reward received from the environment with input from the critic. Plasticity of the projections from inputs to the critic is modulated by this reward prediction error, as described below.

In addition, neurons in the input layer project to a population of neurons representing the available actions (the *actor*). To enforce selection of a specific action, the actor units are arranged in a winner-take-all (WTA) circuit. This is implemented by recurrent connections between actor units that correspond to short-range excitation and long-range inhibition, the distance reflecting the similarity of the action that actor units encode. The activity of actor units is transformed to an action supported by the environment and communicated to the environment via the RMT.

To derive a learning rule for the critic, we follow similar steps as described by Frémaux et al. (2013), but applied to rate models (Equation 1). The critic activity should approximate a continuous-time value function defined by Doya (2000):

$$V^\pi(t) := \int_t^\infty r(s^\pi(t'))e^{-\frac{t'-t}{\tau_r}} dt'. \tag{3}$$

Here, $s(t)$ denotes the state of the agent at time $t$, $r(s^\pi(t))$ denotes the reward obtained in state $s(t)$, $\tau_r$ a discounting factor for future rewards and $\pi$ the agent's policy. To achieve this, we define the following objective function which should be minimized by gradient descent on the weights from inputs to the critic:

$$E(t) := \frac{1}{2}(V^\pi(t) - z(t))^2, \tag{4}$$

where $z(t)$ represents the activity of the critic unit. By performing gradient descent on Equation (4), using a self-consistency equation for $V^\pi(t)$ from the derivative of Equation (3) and bootstrapping on the current prediction for the value (see **Supplementary Material** and Doya, 2000; Frémaux et al., 2013), we obtain the following local Hebbian three-factor learning rule that approximately minimizes the objective function (Equation 4):

$$\Delta w_j = \eta\delta(t)x_j(t)\Theta\left(z(t) - \theta_{\text{post}}\right), \tag{5}$$

where $\eta$ is a learning rate, $x_j(t)$ represents the activity of the $j$th place cell, $\Theta(\cdot)$ the Heaviside function and $\theta_{\text{post}}$ a parameter that accounts for noise on the postsynaptic unit (see **Supplementary Material** for details). The term $\delta(t) = \dot{v}(t) + r(t) - \frac{1}{\tau_r}v(t)$ corresponds to the activity of the reward prediction error unit, acting as a neuromodulatory signal for the Hebbian plasticity between the presynaptic ($x_j$) and postsynaptic ($z$) units. To avoid explicit calculation of the derivative, we approximate $\delta(t)$ by:

$$\delta(t) \approx \left(\frac{1}{d} - \frac{1}{\tau_r}\right)v(t) - \frac{1}{d}v(t-d) + r(t). \tag{6}$$

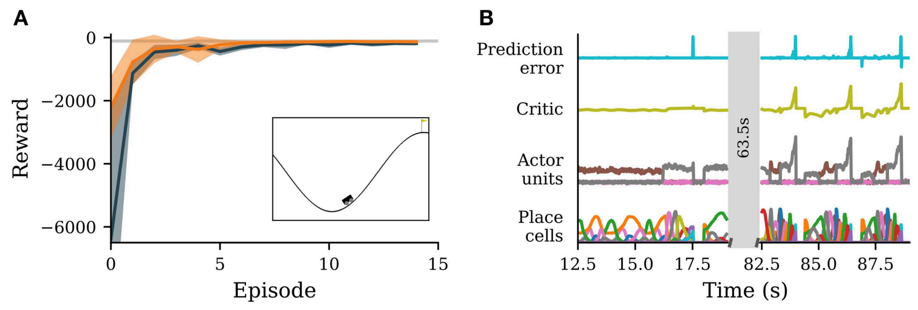

**FIGURE 3 |** A neuronal network simulated in NEST successfully learns to navigate in an environment with continuous states and discrete actions. **(A)** Reward obtained by the agent per episode averaged over 10 simulations with different seeds (solid orange curve). Orange band indicates ± one standard deviation. Dark gray represents the reward obtained from Q-learning. The light gray line marks average reward per episode for which the environment is considered solved. Inset: screenshot of the environment with agent (stylized vehicle), environment with valley and two hills and goal position (yellow flag). The agent is close to a typical starting position at the trough. **(B)** Activity traces of place cells (bottom), actor units (second from bottom), critic unit (second from top) and reward prediction error unit (top). Shown are neural activities during 6.5 s early (left) and late (right) during learning. The neural network simulation was run with a real-time factor of one.

To compute the derivative we hence implement two connections from the critic to the reward-prediction error unit: one instantaneous, and one with delay $d > 0$.

As proposed by Frémaux et al. (2013), to learn an optimal policy, we exploit that the actor units follow the same dynamics as the critic. We hence apply the same learning rule to the connections between the inputs and the actor units. In order to assure that at least one actor unit is active, thus preventing a deadlock, we introduce a minimal weight for each connection between input and output units and add input noise to the actor units.

### 3.3.2. Mountain Car

As an example of an environment with continuous states, we consider the *MountainCar*[8] environment. The task is to steer a toy vehicle that starts at a valley between two hills to the top of the right one (**Figure 3A**, inset). To make the task more challenging, the car's engine is not strong enough to reach the top in one go, so the agent needs to learn to gain momentum by swinging back and forth between the two hills. A single episode in this environment starts when the agent is placed in the valley and ends when it reaches the final position on the top of the right hill. The state of the agent is described by two continuous variables: the x-position $x(t)$ and the x-velocity $\dot{x}(t)$. The agent can choose from three different discrete actions that affect the velocity of the vehicle (accelerate left, no acceleration, accelerate right). It receives punishment (i.e., negative reward) from the environment in every step; the goal is to minimize the total punishment collected over the whole episode. Since it is challenging for a neuronal network implementation of the actor-critic architecture with exclusively excitatory synapses to learn the value function corresponding to a task with solely negative reinforcement (Potjans et al., 2011), we provide additional reward when the agent reaches the final position.

To translate the agent's current state into neuronal activity, we distribute 25 place cells evenly across the two-dimensional plane of possible positions and velocities using the *discretize adapter* of the RMT. The actor is implemented by a WTA circuit of three units as shown in (3.3.1). The activity of these units is transformed into an action via the *argmax adapter* (3.1).

We compare the performance of our neuronal network to Q-learning (Watkins and Dayan, 1992) with function approximation via a multi-layer perceptron (see e.g., Tesauro, 1995; Mnih et al., 2013). The position and velocity of the car are projected to a population of hidden units with rectifying-linear activation function, which in turn project to three output units, encoding the estimated Q-value of each possible action. These Q-values are used by an epsilon-greedy strategy to select the next move. We use the ADAM optimizer (Kingma and Ba, 2014) and memory replay (Lin, 1993) to train the Q-function network (see **Supplementary Material** for details).

Initially, the agent explores the environment by selecting random actions. Due to the WTA circuit dynamics, a single actor neuron stays active over an extended period of time. The constant punishment gradually decreases the weights from the place cells to the corresponding actor unit, eventually leading to another actor unit becoming active (**Figure 3B**, left). After a while, the agent reaches the goal by performing actions that have not been significantly punished. For this task the stable nature of the WTA is advantageous, causing the agent to perform the same action repeatedly allowing efficient exploration of the state space. After the agent has found the goal once, the number of steps spent on exploring actions in the following episodes is much smaller. From the sixth episode on, the performance of the agent is already close to optimal (**Figure 3A**). After learning for about ten episodes, the agent's performance has converged. The value of the final state has been successfully propagated backwards over different states, leading to a ramping of activity of the critic unit from the start of an episode to the end (**Figure 3B**, right).

In comparison to Q-learning, the agent avoids high losses at the start of a training episode. This can most likely be traced back to two factors, which endow our agent with an advantage over Q-learning with function approximation. First, our agent starts with predefined place cells that reliably encode the position

[8]https://gym.openai.com/envs/MountainCar-v0/

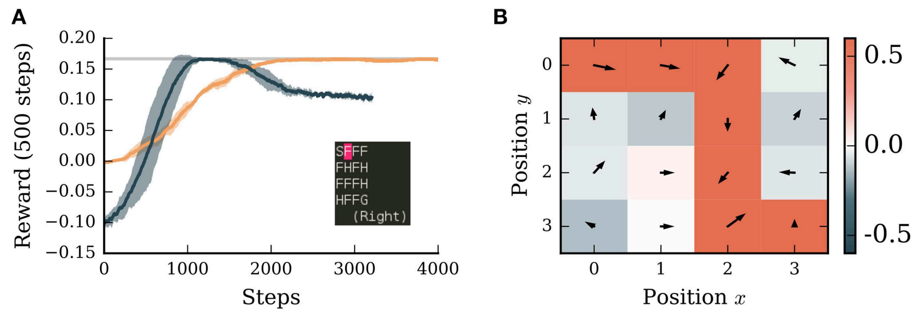

```
SFFF
FHFH
FFFH
HFFG
  (Right)
```

**FIGURE 4 |** A neuronal network simulated in NEST successfully learns to navigate in a grid world with discrete states and discrete actions. **(A)** Orange curve: average reward collected by the agent over the next 500 steps averaged over 5 simulations. Dark blue curve: performance of Potjans et al. (2011) model averaged over 5 simulations. Shaded bands indicates ± one standard deviation. Gray line: theoretical optimum. Inset: screenshot of the environment with start state (S), frozen states (F), holes (H), and goal state (G). The position of the agent is indicated in pink. **(B)** The learned policy and value map of the environment. Red colors indicate positive, blue colors negative values. Arrows indicate the preferred direction of movement. The neural network simulation was run with a real-time factor of two.

in state space and it only has to learn to appropriately combine the activities of these place cells. In contrast, Q-learning starts from a completely blank slate, with no prior knowledge about the input space. It would be incorrect to conclude from this that place cells are generally the superior strategy: manually-defined place cells become infeasible in high-dimensional state spaces as their number increases exponentially in the number of input-space dimensions, whereas Q-learning with function approximation can be scaled to very high-dimensional input spaces (see e.g., Mnih et al., 2013). The second advantage of our agent are long transients in action selection. Before learning the correct sequence of actions, the agent tends to explore a single action for an extended period of time (see trajectories of actor units, **Figure 3B**, left), whereas Q-learning changes action often. For this particular environment sticking to one action for an extended period of time, especially during the early phases of learning, is advantageous as the final strategy involves few action changes (**Figure 3B**, right). This disadvantage can most likely be attenuated by using frame skipping or similar methods (cf. Mnih et al., 2013).

### 3.3.3. Frozen Lake

As a second application illustrating the use of the toolchain for discrete environments, we train the same network model on the *FrozenLake*[9] environment. This consists of a discrete set of 16 states arranged in a four-by-four grid (**Figure 4A**, inset). Each state is either a start state (S), a goal state (G), a hole (H), or a frozen state (F). From the start position, the agent has to reach the rewarded state by navigating over the frozen states without falling into holes which reset the agent to the starting position. In each step the agent can choose from four different actions: move west, move north, move east and move south. Usually, the tiles are "slippery," i.e., there is a chance that a random action is executed irrespective of the action chosen by the agent. However, to simplify learning for demonstration purposes we turn this feature off. Upon reaching the goal the agent receives a reward of magnitude one. Since the optimal path involves six steps from start to goal, the theoretical optimal reward per step is $\sim 0.16$. To encourage exploration the agent receives a small punishment in each state and, additionally, to speed up learning the agent is punished for falling into holes.

Unlike in the continuous *MountainCar* environment, the tuning curves of place cells do not overlap in the discrete case, leading to sharp transitions in the network activity. This leads to severe issues for associating values and actions with the respective states. To address this problem we introduced a simple eligibility trace by evaluating the activity of the pre- and post synaptic units in the learning rule with a small delay $\delta t$ (see **Supplementary Material**). With this addition, the network model is able to find the optimal solution for this task within roughly 2,000 steps (**Figure 4A**). It also learns to associate holes with punishment and frozen states with reward if they are on the path to the goal (**Figure 4B**). Although there are two possible paths to the goal, the agent prefers the path with fewer corners, likely as a consequence of the WTA circuit which tends to select the same action repeatedly.

We compare the performance of our algorithm to an adapted spiking neural network model of the basal ganglia implementing reinforcement learning (Potjans et al., 2011; Jitsev et al., 2012). Learning in this algorithm is faster than our implementation and reaches the optimal solution after only 1,000 steps (**Figure 4A**). However, the performance of the spiking model drops after 2,000 steps to a sub-optimal value. As this model relies on a very high discount factor ($\gamma = 0.99$), which is close to 'infinite horizon', the values of the states saturate in the vicinity to the goal. This can lead to a low contrast of preferred actions in those states and therefore to a sub-optimal policy. To resolve this issue is beyond the scope of this manuscript (see Kato and Morita, 2016 for an investigation of such matters), but underlines the importance of comparing alternative models on the same task. Only through such activities can we identify the strengths and weaknesses of different functional hypotheses and thus make more rapid progress in the field.

## 4. CONCLUSION

In this manuscript, we have argued that standardized benchmarks are of critical importance to compare and improve

[9]https://gym.openai.com/envs/FrozenLake-v0/

functional neural network models. Moreover, to investigate the characteristics of the neural circuits that allow agents to operate autonomously in their environments and learn appropriate behaviors, simulation infrastructure must enable closed-loop interaction between agent and environment.

To make such a set of closed-loop benchmarks available to the computational neuroscience community, we have developed a toolchain that closes the loop between the OpenAI Gym and neural network simulators implementing the MUSIC interface, notably NEST and NEURON. We demonstrated the functionality of the toolchain by implementing an actor-critic architecture in NEST and evaluating its performance on two different environments. The performance of the network quickly reached near-optimal performance on these two tasks.

Compared to creating customized environments within the framework of a neuronal simulator, using readily available, well-tested tools is considerably easier (and thus faster) for the researcher, often computationally more efficient, and most importantly, supports reproducible science. In addition, having the OpenAI Gym environments as common benchmarks in both fields encourages comparison between traditional machine learning and biologically plausible implementations. In contrast to models presented in previous studies, our toolchain makes it easy for other researchers to extend our implementation of an actor-critic architecture to other environments, replace neuron models or explore alternative learning rules. The simulation and visualization scripts to reproduce the results presented for the network model described here are publicly available[10], and so can serve as a starting point for more complex models. In addition a dedicated tutorial introduces the toolchain step-by-step using NEST as an example simulator[11].

While the toolchain currently only supports the OpenAI Gym, the extension to other toolkits is simple due to a modular design of the wrapper. The RMT can be found on GitHub and is available under the GPLv3. The OpenAI Gym ZeroMQ wrapper is also available via GitHub under the MIT license. A complementary development to the work presented here is provided by SPORE, a framework for reward-based learning with spiking neurons in the NEST simulator[12]. It provides support for synapse models with time-driven updates, additional support for recording and evaluating traces of neuronal state variables and introduces MUSIC ports for communicating rewards to a running simulation.

With the work presented here we enable researchers to build more easily upon previous studies and evaluate novel models. We hope this boosts the progress in computational neuroscience in uncovering the biophysical mechanisms involved in autonomous behavior and learning.

[10]https://github.com/INM-6/closed-loop-learning-in-autonomous-agents

[11]https://github.com/INM-6/nestrl-tutorial/

[12]https://github.com/IGITUGraz/spore-nest-module

## DATA AVAILABILITY

The datasets generated for this study can be found on GitHub (https://github.com/INM-6/closed-loop-learning-in-autonomous-agents).

## AUTHOR CONTRIBUTIONS

This study was conceived and designed by JJ, PW, and AM. The toolchain and tested models were implemented by JJ and PW. The simulations were carried out and analyzed by JJ and PW. The manuscript was written jointly by all authors.

## FUNDING

We acknowledge partial support by the German Federal Ministry of Education through our German-Japanese Computational Neuroscience Project (BMBF Grant 01GQ1343), the Helmholtz Alliance through the Initiative and Networking Fund of the Helmholtz Association and the Helmholtz Portfolio theme Supercomputing and Modeling for the Human Brain, and the European Union's Horizon 2020 Framework Programme for Research and Innovation under Specific Grant Agreement Nos. 720270 and 785907 (Human Brain Project SGA1 and SGA2).

## ACKNOWLEDGMENTS

We warmly thank our colleagues in the NEST development team for constructive discussions and support.

## SUPPLEMENTARY MATERIAL

The Supplementary Material for this article can be found online at: https://www.frontiersin.org/articles/10.3389/fncom.2019.00046/full#supplementary-material

## REFERENCES

Abadi, M., Agarwal, A., Barham, P., Brevdo, E., Chen, Z., Citro, C., et al. (2016). Tensorflow: Large-scale machine learning on heterogeneous distributed systems. *arXiv preprint arXiv:1603.04467*.

Aswolinskiy, W., and Pipa, G. (2015). RM-SORN: a reward-modulated self-organizing recurrent neural network. *Front. Comput. Neurosci.* 9:36. doi: 10.3389/fncom.2015.00036

Baladron, J., and Hamker, F. H. (2015). A spiking neural network based on the basal ganglia functional anatomy. *Neural Netw.* 67, 1–13. doi: 10.1016/j.neunet.2015.03.002

Bekolay, T., Bergstra, J., Hunsberger, E., DeWolf, T., Stewart, T. C., Rasmussen, D., et al. (2013). Nengo: a python tool for building large-scale functional brain models. *Front. Neuroinform.* 7:48. doi: 10.3389/fninf.2013.00048

Bellemare, M., Naddaf, Y., Veness, J., and Bowling, M. (2015). "The arcade learning environment: an evaluation platform for general agents," in *Twenty-Fourth International Joint Conference on Artificial Intelligence*.

Bengio, Y., Lamblin, P., Popovici, D., Larochelle, H., et al. (2007). Greedy layer-wise training of deep networks. *Adv. Neural Inform. Process. Syst.* 19:153.

Bower, J. M., and Beeman, D. (2007). GENESIS (simulation environment). *Scholarpedia* 2:1383. doi: 10.4249/scholarpedia.1383

Brockman, G., Cheung, V., Pettersson, L., Schneider, J., Schulman, J., Tang, J., et al. (2016). OpenAI Gym. *ArXiv e-prints. arXiv preprint arXiv:1606.01540*.

Carnevale, T., and Hines, M. (2006). *The NEURON Book*. Cambridge: Cambridge University Press.

Collobert, R., Bengio, S., and Mariéthoz, J. (2002). *Torch: A Modular Machine Learning Software Library.* Technical report, Idiap.

Deng, J., Dong, W., Socher, R., Li, L.-J., Li, K., and Fei-Fei, L. (2009). "ImageNet: a large-scale hierarchical image database," in *CVPR09*.

Djurfeldt, M., Hjorth, J., Eppler, J. M., Dudani, N., Helias, M., Potjans, T. C., et al. (2010). Run-time interoperability between neuronal simulators based on the music framework. *Neuroinformatics* 8, 43–60. doi: 10.1007/s12021-010-9064-z

Doya, K. (2000). Reinforcement learning in continuous time and space. *Neural Comput.* 12, 219–245. doi: 10.1162/089976600300015961

Echeverria, G., Lassabe, N., Degroote, A., and Lemaignan, S. (2011). "Modular open robots simulation engine: Morse," in *2011 IEEE International Conference on Robotics and Automation* (Citeseer), 46–51.

Eppler, J. M., Helias, M., Muller, E., Diesmann, M., and Gewaltig, M. (2009). PyNEST: a convenient interface to the NEST simulator. *Front. Neuroinform.* 2:12. doi: 10.3389/neuro.11.012.2008

Falotico, E., Vannucci, L., Ambrosano, A., Albanese, U., Ulbrich, S., Vasquez Tieck, J. C., et al. (2017). Connecting artificial brains to robots in a comprehensive simulation framework: the neurorobotics platform. *Front. Neurorobot.* 11:2. doi: 10.3389/fnbot.2017.00002

Frémaux, N., Sprekeler, H., and Gerstner, W. (2010). Functional requirements for reward-modulated spike-timing-dependent plasticity. *J. Neurosci.* 30, 13326–13337. doi: 10.1523/JNEUROSCI.6249-09.2010

Frémaux, N., Sprekeler, H., and Gerstner, W. (2013). Reinforcement learning using a continuous time actor-critic framework with spiking neurons. *PLoS Comput. Biol.* 9:e1003024. doi: 10.1371/journal.pcbi.1003024

Friedrich, J., and Lengyel, M. (2016). Goal-directed decision making with spiking neurons. *J. Neurosci.* 36, 1529–1546. doi: 10.1523/JNEUROSCI.2854-15.2016

Friedrich, J., Urbanczik, R., and Senn, W. (2014). Code-specific learning rules improve action selection by populations of spiking neurons. *Int. J. Neural Syst.* 24:1450002. doi: 10.1142/S0129065714500026

Gerstner, W., and Naud, R. (2009). How good are neuron models? *Science* 326, 379–380. doi: 10.1126/science.1181936

Gewaltig, M.-O., and Diesmann, M. (2007). NEST (NEural Simulation Tool). *Scholarpedia* 2:1430. doi: 10.4249/scholarpedia.1430

Goodman, D. F., and Brette, R. (2009). The brian simulator. *Front. Neurosci.* 3, 192–197. doi: 10.3389/neuro.01.026.2009

Hahne, J., Dahmen, D., Schuecker, J., Frommer, A., Bolten, M., Helias, M., et al. (2017). Integration of continuous-time dynamics in a spiking neural network simulator. *Front. Neuroinform.* 11:34. doi: 10.3389/fninf.2017.00034

Hazan, H., Saunders, D. J., Khan, H., Patel, D., Sanghavi, D. T., Siegelmann, H. T., and Kozma, R. (2018). Bindsnet: a machine learning-oriented spiking neural networks library in python. *Front. Neuroinform.* 12:89. doi: 10.3389/fninf.2018.00089

Hintjens, P. (2013). *ZeroMQ: Messaging for Many Applications*. O'Reilly Media, Inc.

Hinton, G., Deng, L., Yu, D., Dahl, G. E., Mohamed, A.-R., Jaitly, N., et al. (2012). Deep neural networks for acoustic modeling in speech recognition: the shared views of four research groups. *IEEE Signal Process. Mag.* 29, 82–97. doi: 10.1109/MSP.2012.2205597

Hinton, G. E., and Salakhutdinov, R. R. (2006). Reducing the dimensionality of data with neural networks. *Science* 313, 504–507. doi: 10.1126/science.1127647

Hinton, G. E., Srivastava, N., Krizhevsky, A., Sutskever, I., and Salakhutdinov, R. R. (2012). Improving neural networks by preventing co-adaptation of feature detectors. *arXiv preprint arXiv:1207.0580*.

Human Brain Project (2014). *Project Website.* Available online at: http://www.humanbrainproject.eu

Izhikevich, E. M. (2007). Solving the distal reward problem through linkage of STDP and dopamine signaling. *Cereb. Cortex* 17, 2443–2452. doi: 10.1093/cercor/bhl152

James, B., Olivier, B., Frédéric, B., Pascal, L., and Razvan, P. (2010). "Theano: a CPU and GPU math expression compiler," in *Proceedings of the Python for Scientific Computing Conference (SciPy)*.

Jia, Y., Shelhamer, E., Donahue, J., Karayev, S., Long, J., Girshick, R., et al. (2014). Caffe: convolutional architecture for fast feature embedding. *arXiv preprint arXiv:1408.5093*. doi: 10.1145/2647868.2654889

Jitsev, J., Morrison, A., and Tittgemeyer, M. (2012). "Learning from positive and negative rewards in a spiking neural network model of basal ganglia," in *The 2012 International Joint Conference on Neural Networks (IJCNN)* (IEEE), 1–8.

Jordan, J., Ippen, T., Helias, M., Kitayama, I., Sato, M., Igarashi, J., et al. (2018). Extremely scalable spiking neural network simulation code: from laptops to exascale computers. *Front. Neuroinform.* 12:2. doi: 10.3389/fninf.2018.00034

Kato, A., and Morita, K. (2016). Forgetting in reinforcement learning links sustained dopamine signals to motivation. *PLoS Comput. Biol.* 12:e1005145. doi: 10.1371/journal.pcbi.1005145

Kingma, D. P., and Ba, J. (2014). Adam: a method for stochastic optimization. *arXiv preprint arXiv:1412.6980*.

Koenig, N., and Howard, A. (2004). "Design and use paradigms for gazebo, an open-source multi-robot simulator," in *2004 IEEE/RSJ International Conference on Intelligent Robots and Systems (IROS)(IEEE Cat. No. 04CH37566), Vol. 3* (IEEE), 2149–2154.

Krizhevsky, A., and Hinton, G. (2009). *Learning Multiple Layers of Features From Tiny Images.* Technical Report 4, University of Toronto.

Krizhevsky, A., Sutskever, I., and Hinton, G. E. (2012). "Imagenet classification with deep convolutional neural networks," in *Advances in Neural Information Processing Systems*, 1097–1105.

Kunkel, S., Schmidt, M., Eppler, J. M., Plesser, H. E., Masumoto, G., Igarashi, J., Ishii, S., et al. (2014). Spiking network simulation code for petascale computers. *Front. Neuroinform.* 8:78. doi: 10.3389/fninf.2014.00078

LeCun, Y. (1998). The MNIST Database of Handwritten Digits. Available online at: http://yann.lecun.com/exdb/mnist

Lin, L.-J. (1993). *Reinforcement Learning for Robots Using Neural Networks.* Technical report, Carnegie-Mellon Univ Pittsburgh PA School of Computer Science.

Michel, O. (2004). Cyberbotics Ltd. Webots$^{TM}$ : professional mobile robot simulation. *Int. J. Adv. Robot. Syst.* 1:5. doi: 10.5772/5618

Mnih, V., Badia, A. P., Mirza, M., Graves, A., Lillicrap, T., Harley, T., et al. (2016). "Asynchronous methods for deep reinforcement learning," in *Int. Conf. Mach. Learn.* 1928–1937.

Mnih, V., Kavukcuoglu, K., Silver, D., Graves, A., Antonoglou, I., Wierstra, D., et al. (2013). Playing atari with deep reinforcement learning. *arXiv preprint arXiv:1312.5602*.

Mnih, V., Kavukcuoglu, K., Silver, D., Rusu, A. A., Veness, J., Bellemare, M. G., et al. (2015). Human-level control through deep reinforcement learning. *Nature* 518, 529–533. doi: 10.1038/nature14236

Moren, J., Sugimoto, N., and Doya, K. (2015). Real-time utilization of system-scale neuroscience models. *J. Jap. Neural Netw. Soc.* 22, 125–132. doi: 10.3902/jnns.22.125

Moser, E. I., Kropff, E., and Moser, M.-B. (2008). Place cells, grid cells, and the brain's spatial representation system. *Annu. Rev. Neurosci.* 31, 69–89. doi: 10.1146/annurev.neuro.31.061307.090723

Paszke, A., Gross, S., Chintala, S., Chanan, G., Yang, E., DeVito, Z., et al. (2017). Automatic Differentiation in Pytorch.

Potjans, W., Diesmann, M., and Morrison, A. (2011). An imperfect dopaminergic error signal can drive temporal-difference learning. *PLoS Comput. Biol.* 7:e1001133. doi: 10.1371/journal.pcbi.1001133

Potjans, W., Morrison, A., and Diesmann, M. (2009). A spiking neural network model of an actor-critic learning agent. *Neural Comput.* 21, 301–339. doi: 10.1162/neco.2008.08-07-593

Quigley, M., Conley, K., Gerkey, B., Faust, J., Foote, T., Leibs, J., et al. (2009). "ROS: an open-source Robot Operating System," in *ICRA Workshop on Open Source Software, Vol. 3* (Kobe).

Raina, R., Madhavan, A., and Ng, A. Y. (2009). "Large-scale deep unsupervised learning using graphics processors," in *Proceedings of the 26th Annual International Conference on Machine Learning* (ACM), 873–880.

Rasmussen, D., and Eliasmith, C. (2014). "A neural model of hierarchical reinforcement learning," in *CogSci*.

Rombouts, J. o., Bohte, S. M., and Roelfsema, P. R. (2015). How attention can create synaptic tags for the learning of working memories in sequential tasks. *PLoS Comput. Biol.* 11:e1004060. doi: 10.1371/journal.pcbi.1004060

Rueckert, E., Kappel, D., Tanneberg, D., Pecevski, D., and Peters, J. (2016). Recurrent spiking networks solve planning tasks. *Sci. Rep.* 6:21142. doi: 10.1038/srep21142

Russakovsky, O., Deng, J., Su, H., Krause, J., Satheesh, S., Ma, S., et al. (2015). ImageNet large scale visual recognition challenge. *Int. J. Comput. Vis.* 115, 211–252. doi: 10.1007/s11263-015-0816-y

Sanz Leon, P., Knock, S. A., Woodman, M. M., Domide, L., Mersmann, J., McIntosh, A. R., et al. (2013). The virtual brain: a simulator of primate brain network dynamics. *Front. Neuroinform.* 7:10. doi: 10.3389/fninf.2013.00010

Sheik S., and Liu, Q. (2019). *SINABS - A Spiking Deep Neural Network Inference Emulator*. doi: 10.5281/zenodo.3218477

Silver, D., Huang, A., Maddison, C. J., Guez, A., Sifre, L., Van Den Driessche, G., et al. (2016). Mastering the game of go with deep neural networks and tree search. *Nature* 529, 484–489. doi: 10.1038/nature16961

Sutton, R. S., and Barto, A. G. (1998). *Reinforcement Learning: An Introduction*. Adaptive Computation and Machine Learning. The MIT Press.

Tesauro, G. (1995). Temporal difference learning and TD-gammon. *Commun. ACM* 38, 58–68.

Todorov, E., Erez, T., and Tassa, Y. (2012). "Mujoco: a physics engine for model-based control," in *2012 IEEE/RSJ International Conference on Intelligent Robots and Systems (IROS)*, 5026–5033.

Urbanczik, R., and Senn, W. (2009). Reinforcement learning in populations of spiking neurons. *Nat. Neurosci.* 12:250. doi: 10.1038/nn.2264

Vasilaki, E., Frémaux, N., Urbanczik, R., Senn, W., and Gerstner, W. (2009). Spike-based reinforcement learning in continuous state and action space: when policy gradient methods fail. *PLoS Comput. Biol.* 5:e1000586. doi: 10.1371/journal.pcbi.1000586

Watkins, C. J., and Dayan, P. (1992). Q-learning. *Mach. Learn.* 8, 279–292.

Watkins, C. J. C. H. (1989). *Learning from delayed rewards* (Ph.D. thesis). University of Cambridge.

Weidel, P., Djurfeldt, M., Duarte, R. C., and Morrison, A. (2016). Closed loop interactions between spiking neural network and robotic simulators based on music and ros. *Front. Neuroinform.* 10:31. doi: 10.3389/fninf.2016.00031

Wils, S., and De Schutter, E. (2009). STEPS: modeling and simulating complex reaction-diffusion systems with Python. *Front. Neuroinform.* 3:15. doi: 10.3389/neuro.11.015.2009

Wilson, M. (2002). Six views of embodied cognition. *Psychon. Bull. Rev.* 9, 625–636. doi: 10.3758/BF03196322

**Conflict of Interest Statement:** The authors declare that the research was conducted in the absence of any commercial or financial relationships that could be construed as a potential conflict of interest.